Molecular dynamics calculations of the thermal expansion properties and melting points of Si and Ge

Molecular dynamics calculations of the thermal expansion properties and melting points of Si and Ge

V Timon, S Brand, S J Clark and R A Abram

Department of Physics, University of Durham, South Road, Durham DH1 3LE, UK

E-mail: v.t.salinero@durham.ac.uk

Abstract
The thermal expansion properties and melting points of silicon and germanium are calculated using molecular dynamics simulations within the density functional theory framework. An isothermal–isobaric (NPT) ensemble is considered in a periodic system with a relatively small number of particles per unit cell to obtain the thermal expansion data over a range of temperatures, and it is found that the calculated thermal expansion coefficients and bond lengths agree well with experimental data. Also, the positions of discontinuities in the potential energy as a function of temperature are in good agreement with the experimental melting points.

(Some figures in this article are in colour only in the electronic version)

1. Introduction and method

Si and Ge are both tetrahedrally bonded semiconductors, with Si of particularly great importance for microelectronic devices and circuits, while SiGe alloys are finding growing uses in similar applications. The thermal expansion properties of Si and Ge are well known from experiment [1–3] at low and high temperature but there is also an interest in understanding their theoretical basis. Knowledge of the thermal expansion coefficients of these materials is very important for understanding the nature of the stress in device structures [4]. The coefficients can be theoretically obtained via a phonon mode Gruneisen parameter model [5] or with the use of a molecular dynamics (MD) simulation. MD is now used as a standard tool with the potential to accurately predict the thermal expansion and melting points of Si and Ge [6–9]. However, a common feature of many of these calculations is the employment of unit cells composed of hundreds of atoms, which leads to high computational cost, and they are therefore restricted to a limited $k = 0$ sampling point scheme, tight-binding methods, etc. In addition, until recently [10] the predicted melting points have been up to several hundred degrees different from experiment [7].

In this work a single-phase molecular dynamic simulation of the solid state is made to study the temperature dependence of the lattice constants for Si and Ge crystals, employing various cell sizes in order to check the consistency of the results. We have considered both Ge and Si over a large temperature range spanning the experimental melting points in order to calculate the thermal expansion coefficients and make some comments concerning the estimation of the melting point at normal atmospheric constant pressure (1 atm).

The *ab initio* code employed here is implemented in the CASTEP V 3.0 package [11], using forces generated by the solution of the Kohn–Sham equations [12] for an extended solid, and provides structural information about the system. Newton's equations of motion for the ions were integrated at a constant time step of 0.002 ps for a single unit cell with Ge or Si atoms for a total thermalization time of 5000 time steps. Vanderbilt ultrasoft pseudopotentials [13] describe the electron–ion interactions. The wavefunctions were expanded in a plane-wave basis set up to an energy cut-off of 400 eV and integrations over the Brillouin zone were performed using a $2 \times 2 \times 2$ Monkhorst–Pack set sampling point scheme [14]. In the case of Ge the 3d electrons were treated as valence electrons. A local-density-approximation (LDA) [15] parametrization is used to calculate the total and potential energies as a function of cell parameters. Calculations were performed in the range of temperatures from 10 to $\sim$2000 K. The method employed to define a temperature, T, and further discussion of the finite temperature approach in this context is described in the works of Nose and Hoover [16, 17]. Partial occupancy of excited states and Gaussian smearing techniques to include contributions at non-zero temperature are employed.

The potential energy and enthalpy of the system increase with temperature because the particles sample higher energy configurations and in condensed matter the attractive force between the atoms or molecules is described by their potential energy relative to the free particle state. In first-order phase transitions (solid–liquid, vapour–liquid and solid–vapour) there is a discontinuity in the enthalpy, entropy and volume at a specific temperature while in the case of second order phase transitions enthalpy, entropy and volume change continuously but there is a discontinuity in their first derivative with respect to temperature. Hence, a discontinuity in the potential energy of the system as a function of temperature can indicate the presence of a phase transition.

2. Results

A series of simulations has been carried out beginning with systems consisting of the bulk solid phase structure of Si and Ge, with cell parameters and atom positions optimized by means of total energy calculations. Then, using MD simulations the system was heated to temperatures below and above the known experimental melting points.

In our calculations, we use supercells of various sizes to check for any significant effects associated with the finite number of atoms in the supercell. In *ab initio* calculations it has been common to use supercells containing up to hundreds of atoms, which appear to lead to reasonably converged results. However, in this work we perform calculations with smaller cell sizes of eight and 16 atoms, as well as a 54-atom (rhombohedral) supercell in the case of germanium. Somewhat unexpectedly, we find rather good results even with a very small cell, as will be described below.

In particular, we have been interested in the thermal expansion coefficients of the materials. By definition the coefficient of thermal expansion for length, area or volume is the ratio of the change in length, area or volume per unit change in temperature. In the case of the linear thermal expansion coefficient, α, we take this to be given by the expression $\alpha = \frac{1}{l_0} \frac{dl}{dT}$, where l_0 is the length at an appropriate reference temperature and l is the T-dependent value [18]. In

Table 1. Calculated lattice constants, thermal expansion coefficients and potential energy of silicon.

Temperature (K)	Lattice constant a (Å)	Std error in the mean	Potential energy (eV)	Std error in the mean	α_a (10^{-6} K^{-1})
10	5.396 04	0.000 0283	−1178.4300	0.000 0498	
25	5.396 54	0.000 1252	−1178.4100	0.000 1332	
55	5.396 79	0.000 1072	−1178.3800	0.000 3111	
75	5.398 18	0.000 1669	−1178.3500	0.000 4193	
90	5.398 46	0.000 2616	−1178.3400	0.000 5120	
100	5.399 31	0.000 2304	−1178.3300	0.000 4566	
200	5.401 83	0.000 3819	−1178.2100	0.000 9882	1.6391
400	5.405 66	0.000 4650	−1177.9900	0.001 8680	2.6006
550	5.406 25	0.000 5573	−1177.8200	0.002 2615	3.2684
700	5.408 31	0.000 6430	−1177.6500	0.003 4099	3.8773
800	5.410 04	0.000 6870	−1177.5000	0.004 7063	4.2458
1000	5.413 69	0.000 8753	−1177.2600	0.005 4893	4.8851
1200	5.422 78	0.000 8654	−1177.0400	0.005 5941	5.3875
1510	5.431 96	0.000 6878	−1176.5900	0.009 1796	5.8981
1625	5.433 78	0.001 3199	−1176.4200	0.010 3752	6.0098
1648	5.435 09	0.001 4083	−1176.4000	0.013 2278	
1700	5.170 54	0.002 2292	−1175.6900	0.011 5494	
1800	5.211 35	0.002 4739	−1175.4300	0.014 4626	
1925	5.255 88	0.003 3783	−1175.1800	0.021 9992	

our simulations l equates to the Si and Ge lattice constant, a, which we calculate at a series of values of T.

The average values of the lattice constant a and potential energy obtained from a full geometric structural relaxation were recorded at every step of the simulation and the calculated thermal expansion coefficients are shown in tables 1 and 2. In the case of the Ge supercell, table 2(b), the value of both the supercell lattice constant and the corresponding conventional cubic unit cell lattice constant are shown. The estimated errors are obtained from the standard deviation of all the values calculated per time step. With these values the data are fitted to obtain an analytic function to describe the evolution of the cell parameter with temperature.

At low temperatures a common characteristic of tetrahedrally bonded solid Si and Ge is the existence of regions with negative thermal expansion coefficients at a temperature of approximately $T/\theta_D = 0.2$, where θ_D is the Debye temperature [3]. This is a problem region in our calculations due to their sensitivity and associated relatively large errors at low T; this affects our ability to make a reliable fit to the results. Thus we have not fitted the data at temperatures below 100 K when calculating the thermal expansion coefficients. We note that the existence of negative thermal expansion coefficients also causes problems in, for example, Grüneisen model predictions of α below about 200 K [19]. Our calculated results (excluding the problematic region) for the lattice constant as a function of temperature and the associated fits to the data are shown in figure 1 for Si in the range 100–1648 K, and in figure 2 for Ge in the range 100–1180 K.

In order to compare our calculated results with those of experiment we show our fitted curves of lattice parameter as a function of temperature together with the available experimental results at normal pressure (1 atm) in figures 3 and 4. In figure 3 our fit for Si is compared to the experimental results of Yim and Paff [20] and figure 4 compares our Ge fit to the experimental results of Singh [21] over the relevant temperature ranges. We note that the initial differences between the experimental and calculated values of the lattice constants is typical of the errors

Table 2. Calculated lattice constants, thermal expansion coefficients and potential energy of germanium.

(a) Ge eight-atom cubic unit cell

Temperature (K)	Lattice constant a (Å)	Std error in the mean	Potential energy (eV)	Std error in the mean	α_a (10^{-6} K^{-1})
10	5.618 110	0.000 207	−2165.67	7.93E−005	
25	5.618 710	0.000 237	−2165.65	0.000 219	
55	5.619 620	0.000 181	−2165.62	0.000 369	
100	5.621 490	0.000 278	−2165.57	0.000 718	
200	5.622 300	0.000 386	−2165.44	0.001 818	1.9281
300	5.626 620	0.000 504	−2165.32	0.002 274	6.7034
500	5.631 130	0.000 523	−2165.06	0.003 451	9.3027
550	5.636 260	0.000 486	−2165.05	0.003 492	9.5211
700	5.647 620	0.000 743	−2164.86	0.004 149	9.8808
800	5.650 810	0.000 972	−2164.74	0.003 769	9.9993
925	5.658 680	0.000 860	−2164.61	0.004 190	10.0087
1000	5.664 480	0.000 906	−2164.49	0.004 541	10.1213
1180	5.670 630	0.001 131	−2164.26	0.006 191	
1220	5.549 000	0.002 315	−2164.11	0.007 125	
1300	5.552 369	0.002 563	−2164.00	0.007 852	
1400	5.608 900	0.002 537	−2163.90	0.007 956	
1600	5.563 770	0.003 120	−2163.70	0.008 125	

(b) Ge 16-atom supercell

Temperature (K)	Supercell lattice constant (Å)	Cubic unit cell lattice constant a (Å)	Std error in the mean	Potential energy (eV)	Std error in the mean	α_a (10^{-6} K^{-1})
25	7.936 850	5.6122	0.000 067	−4333.44	0.000 221	
50	7.936 840	5.6122	0.000 131	−4333.38	0.000 481	
100	7.936 480	5.6119	0.000 221	−4333.31	0.000 892	
200	7.937 930	5.6130	0.000 351	−4333.03	0.002 325	6.9973
250	7.944 880	5.6178	0.000 451	−4332.93	0.002 129	7.2646
400	7.948 680	5.6206	0.000 479	−4332.78	0.002 425	7.4384
500	7.958 951	5.6278	0.000 611	−4332.38	0.003 303	7.4602
700	7.971 510	5.6367	0.000 767	−4331.89	0.005 196	7.4729
900	7.979 480	5.6424	0.000 852	−4331.35	0.006 230	7.4763
1000	7.987 880	5.6483	0.000 879	−4331.08	0.007 962	7.4771
1125	7.990 100	5.6500	0.000 932	−4331.01	0.008 254	7.4777
1180	7.996 930	5.6554	0.000 990	−4330.75	0.009 044	
1220	7.787 350	5.5053	0.001 595	−4327.13	0.011 550	
1300	7.782 320	5.5053	0.001 630	−4326.75	0.011 567	
1400	7.784 220	5.5043	0.001 802	−4326.59	0.011 905	
1500	7.820 800	5.5301	0.001 752	−4326.27	0.013 807	

encountered in first principles calculations using DFT. In the case of silicon, a calculation involving only an eight-atom supercell is sufficient to give good agreement with experiment when comparing the change in lattice constant with temperature. In the case of Ge, with the additional 3d electrons included as valence electrons, we have performed calculations with eight- and 16-atom supercells, and to a more limited extent with a 54-atom supercell. In figure 4 the slope of the curve for the 16-atom Ge results differs by only about 1% from the experimental value, a significant improvement on the eight-atom results. We note that a
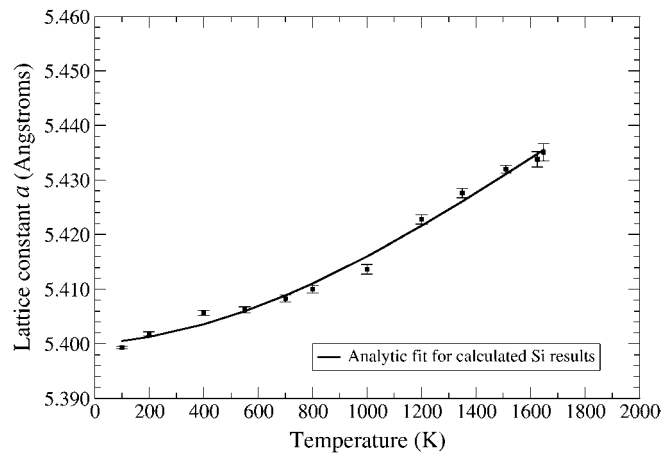
Figure 1. Values calculated from the numerical simulations (data points) and fitted curve for the lattice constant a, as a function of temperature for Si.
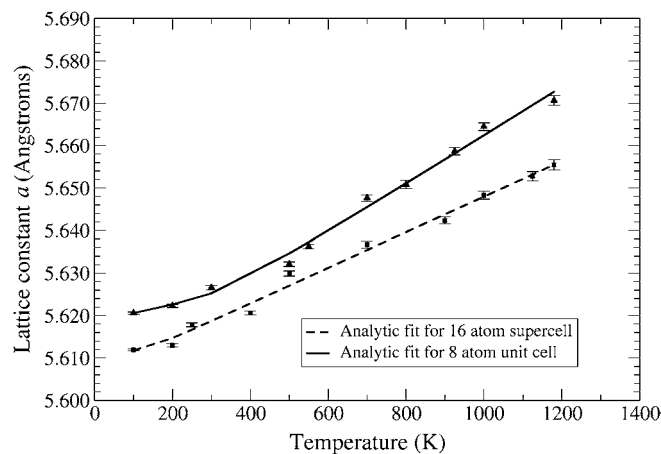

Figure 2. Values calculated from the numerical simulations (data points) and fitted curves for the lattice constant a, as a function of temperature for Ge.

linear extrapolation of the eight- and 16-atom data to $T = 0$ K leads to a consistent value for the zero-temperature lattice constant. To investigate the convergence properties further in the Ge case, more computationally expensive calculations with a 54-atom supercell were carried out for several sample temperatures. These calculations gave lattice constant values of 5.616, 5.629 and 5.645 Å at temperatures of 100, 500 and 1000 K respectively. There is again a small systematic shift in the overall results but these values differ only slightly from those for the 16-atom unit cell despite the significantly increased computational expense and this justifies the use of the smaller, 16-atom, supercell in the case of Ge. This difference in the minimum size system between Si and Ge may be due to the ion mobility difference observed for Si and Ge [22]. It is also possible that the inclusion of the d electrons could have some influence, and consequently the larger cell size required in the case of Ge may be indicative of that required for materials such as GaAs and GaN, for example. In summary, these results give us a good indication of the reliability of the calculations and confidence in the calculated values of α using
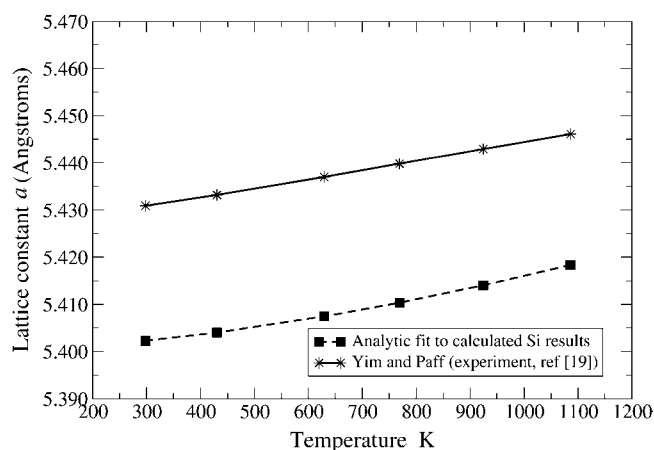
Figure 3. Calculated and experimental values of the Si lattice parameter as a function of temperature.
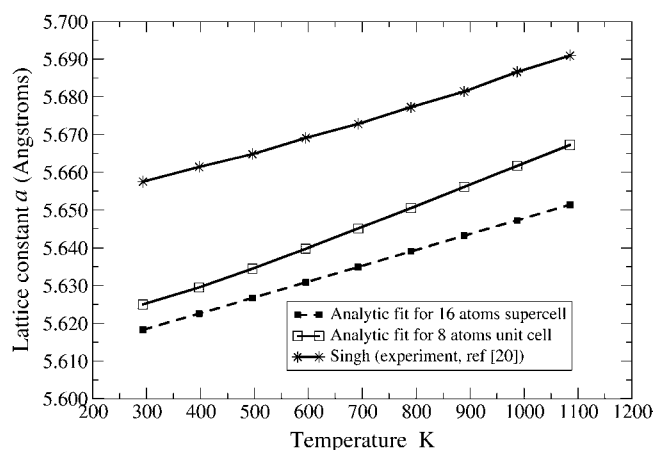

Figure 4. Calculated and experimental values of the Ge lattice parameter as a function of temperature.

an eight-atom unit cell in the case of silicon, and a 16-atom unit cell in the case of germanium. Use of a bigger unit cell does not significantly improve the agreement with experiment, and in particular the value of the thermal expansion coefficient, α.

With the analytic fits to the results we were able to obtain calculated values for the thermal expansion coefficients. These functions were then used (with a_0 being the value of a at 100 K) to obtain the thermal expansion coefficients between 100 K and temperatures close to the melting points as listed in the last column in tables 1 and 2. Figures 5 and 6 show the comparison between the thermal expansion coefficients calculated from first principles and those measured by experiment [18]. According to figures 5 and 6 the calculations for Si and Ge give results which are consistent with the experimental data. In the case of Ge the results are somewhat improved with the use of the 16-atom supercell as compared to the eight-atom supercell. In each case we can see that the calculated data reproduces the same type of behaviour as seen in experiment. For both Si and Ge the increase in the thermal expansion coefficient tends to level off with increased temperature, consistent with experiment.
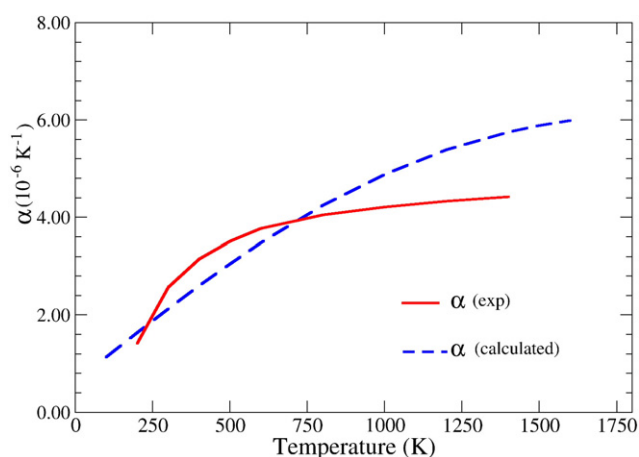
Figure 5. Comparison of the calculated and experimental linear thermal expansion coefficients of Si versus temperature.
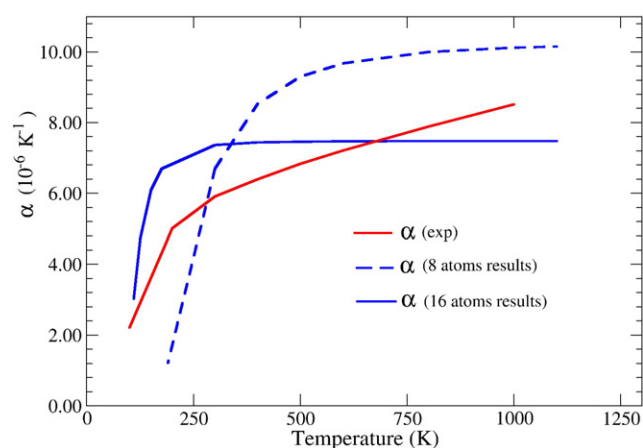

Figure 6. Comparison of the calculated and experimental linear thermal expansion coefficients of Ge versus temperature.

An interesting observation concerning this work relates to the identification of a first order phase transition in Si and Ge. Previous detailed studies reported by Sugino and Car [7] and Alfe and Gillan [10] have modelled the phase transformation of Si from first principles employing large unit cells consisting of up to 250 atoms. In our calculations, employing a much smaller number of atoms, we note that in the plots of lattice constant versus temperature there is a discontinuity at elevated temperatures. Although the size of the discontinuity has not been demonstrated to converge in our calculations, its position is relatively independent of the size of the system and appears to coincide with the experimental melting point to within a few degrees. This is demonstrated in figures 7 (Si) and 8 (Ge) where the calculated value of the potential energy is plotted against temperature. It can be seen that this function has two apparent linear regions together with a clear discontinuity between them. The positions of these two discontinuities correlates well with the experimental values of the melting points of Si and Ge respectively. In Si, the discontinuity occurs at 1674 ± 26 K in good agreement with the experimental melting point $T_{\mathrm{m}} = 1685$ K [10], whereas for Ge it occurs at 1200 ± 20 K,
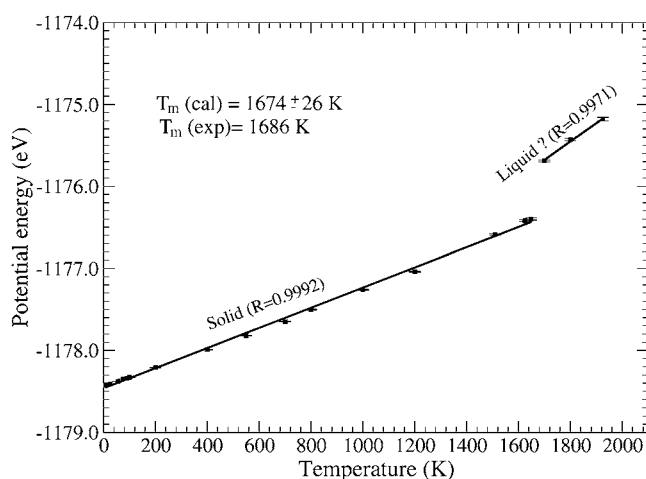
Figure 7. Calculated potential energy as a function of the temperature for Si.

Table 3. Volume and fractional change in volume calculated at the discontinuity in potential energy for Si and Ge.

Element	State	Temperature	Volume (Å^3)	$\Delta V/V_s$ (calc.)	$\Delta V/V_s$ (exp.)
Si	Solid	1648	$160.65 \pm 0.125\,473$		
Si	Phase change	1700	$138.42 \pm 0.177\,409$		
				$\sim 13.8\%$	11.9% [a]
Ge (unit cell)	Solid	1180	$182.45 \pm 0.105\,826$		
Ge (unit cell)	Phase change	1220	$171.03 \pm 0.141\,716$		
Eight-atom cell				$\sim 6.2\%$	5% [b]
Ge (primitive supercell)	Solid	1180	$360.354 \pm 0.134\,17$		
Ge (primitive supercell)	Phase change	1220	$334.107 \pm 0.208\,35$		
16-atom supercell				$\sim 7.0\%$	5% [b]

[a] Reference [7].
[b] Reference [21].

in good agreement with the experimental value of Ge, $T_m = 1210$ K [23]. This discontinuity in the case of Ge is even more distinct with the use of the 16-atom supercell, but there is no significant change in the position of the discontinuity compared to the eight-atom results.

Other evidence for a structural change relates to anomalies in the cell parameters above the discontinuity as shown in tables 1 and 2. It is known that silicon and germanium liquids are denser than the corresponding solid, in common with a number of elements [24], and also the most familiar example, water. In accord with this phenomenon, both materials show a contraction in volume upon melting quantified by the ratio $\Delta V/V_s$, where ΔV is the decrease in volume of the solid phase with respect to the liquid and V_s is the volume of the material in the solid phase at the transition. The theoretical volume discontinuity from our results is compared with the experimental results for Ge and Si in table 3. The calculated values agree well with the experimental results given in [7, 23] and overall show the same kind of behaviour as is found for Ge and Si at normal pressure [25].

3. Conclusions

In general, we find that our calculated values of the lattice constants and thermal expansion coefficients of silicon and germanium as a function of temperature are in good agreement with
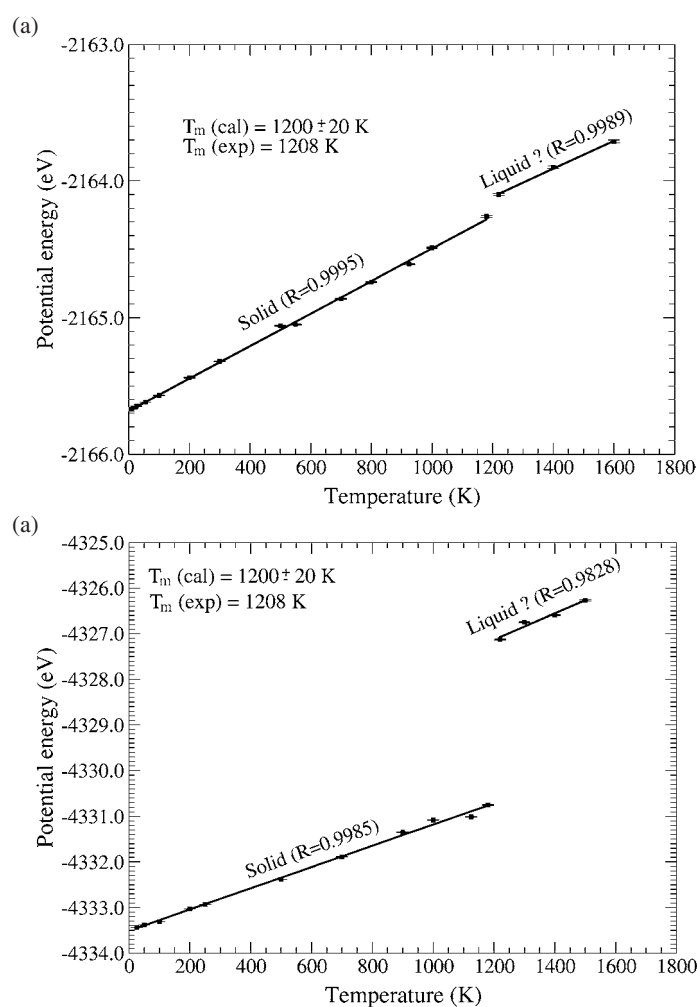
(a)

(a)

Figure 8. Calculated potential energy as a function of temperature for Ge. (a) Ge eight-atom cubic unit cell; (b) Ge 16-atom supercell.

experiment, even though we have employed rather small supercells in the simulation. The calculations also appear to give a good indication of the value of the melting points of the two materials. The use of a small unit cell does, however, involve a trade-off. There are other thermodynamic quantities, such as the latent heat, which cannot be convergently calculated.

Our results suggest that the molecular dynamics simulations based on DFT and LDA and the NPT ensemble is a useful methodology to simulate Si and Ge and by implication other semiconductors also at constant temperature and pressure without the necessity to employ a system involving perhaps some hundreds of atoms.

Acknowledgment

References

[1] Yim W M and Paff R J 1974 *J. Appl. Phys.* **45** 1456
[2] Singh H P 1968 *Acta Crystallogr.* **24** 469
[3] Sparks P W and Swenson C A 1967 *Phys. Rev.* **163** 779
[4] Yamamoto N, Horinaka H and Miyauchi T 1977 *Japan. J. Appl. Phys.* **18** 225
[5] Fabian J and Allen P B 1997 *Phys. Rev. Lett.* **79** 1885
[6] Buda F, Car R and Parinello M 1990 *Phys. Rev.* B **41** 1680
[7] Sugino O and Car R 1995 *Phys. Rev. Lett.* **74** 1823
[8] Horsfieldt A P and Clancy P 1994 *Modelling Simul. Mater. Sci. Eng.* **2** 277
[9] Bernstein N, Mehl M J and Papaconstantopoulos D A 2002 *Phys. Rev.* B **66** 75212
[10] Alfe D and Gillan M J 2003 *Phys. Rev.* B **68** 202512
[11] Segall M D, Lindan P J D, Probert M J, Pickard C J, Hasnip P J, Clark S J and Payne M C 2002 *J. Phys.: Condens. Matter* **14** 2717
[12] Kohn L J and Sham L J 1965 *Phys. Rev.* A **140** 1133
[13] Vanderbilt D 1990 *Phys. Rev.* B **41** 7892
[14] Monkhorst H J and Pack J D 1976 *Phys. Rev.* B **13** 5188
[15] Hohenberg P and Kohn W 1964 *Phys. Rev.* B **136** 864
     Kohn W and Sham L J 1965 *Phys. Rev.* A **137** 1697
[16] Nose S 1984 *Mol. Phys.* **52** 255
[17] Hoover W G 1984 *Phys. Rev.* A **31** 1695
[18] Slack G A and Bartram S F 1975 *J. Appl. Phys.* **46** 89
[19] Reeber R R and Wang K 2000 *J. Mater. Res.* **15** 40
[20] Yim W M and Paff R J 1974 *J. Appl. Phys.* **45** 1456
[21] Singh H P 1968 *Acta Crystallogr.* **24** 469
[22] Shvartsburg A A, Liu B, Lu Z-Y, Wang C-Z, Jarrold M F and Ho K-M 1999 *Phys. Rev. Lett.* **83** 2167
[23] Hall H T 1955 *J. Phys. Chem.* **59** 1144
[24] Young D A 1991 *Phase Diagrams of the Elements* (Berkeley, CA: University of California Press)
     Eisenberg D and Kauzmann W 1969 *The Structure and Properties of Water* (Oxford: Clarendon)
[25] Warren G L and Evenson W E 1975 *Phys. Rev.* B **11** 2979–89